



Citation for published version:

Wagner, J, Le, C, Ting, V & Chuck, C 2017, 'Design and operation of an inexpensive, laboratory-scale, continuous hydrothermal liquefaction reactor for the conversion of microalgae produced during wastewater treatment', *Fuel Processing Technology*, vol. 165, pp. 102-111. <https://doi.org/10.1016/j.fuproc.2017.05.006>

DOI:

[10.1016/j.fuproc.2017.05.006](https://doi.org/10.1016/j.fuproc.2017.05.006)

Publication date:

2017

Document Version

Peer reviewed version

[Link to publication](#)

Publisher Rights

CC BY-NC-ND

University of Bath

Alternative formats

If you require this document in an alternative format, please contact:
openaccess@bath.ac.uk

General rights

Copyright and moral rights for the publications made accessible in the public portal are retained by the authors and/or other copyright owners and it is a condition of accessing publications that users recognise and abide by the legal requirements associated with these rights.

Take down policy

If you believe that this document breaches copyright please contact us providing details, and we will remove access to the work immediately and investigate your claim.

1 **Design and operation of an inexpensive, laboratory-scale,**
2 **continuous hydrothermal liquefaction reactor for the**
3 **conversion of microalgae produced during wastewater**
4 **treatment**

5

6 *Jonathan L. Wagner,^{a,b} Chien D. Le,^c Valeska P. Ting,^d Christopher J. Chuck^{b*}*

7

8 ^a Centre for Doctoral Training in Sustainable Chemical Technologies, Department of Chemical
9 Engineering, University of Bath, Claverton Down, Bath, United Kingdom, BA2 7AY.

10 ^b Department of Chemical Engineering, University of Bath, Claverton Down, Bath, United
11 Kingdom, BA2 7AY.

12 ^c Department of Oil Refining and Petrochemistry, Hanoi University of Mining and Geology,
13 Hanoi, Vietnam

14 ^d Department of Mechanical Engineering, University of Bristol, Bristol BS8 1TR, UK

15

16

17 **Abstract**

18 Recently, much research has been published on the hydrothermal liquefaction (HTL) of
19 microalgae to form bio-crude, which can be further upgraded into sustainable 3rd generation
20 biofuels. However, most of these studies have been conducted in batch reactors, which are not
21 fully applicable to large-scale industrial production. In this investigation an inexpensive laboratory
22 scale continuous flow system was designed and tested for the liquefaction of microalgae
23 produced during wastewater treatment. The system was operated at a range of temperatures

24 (300 °C – 340 °C) and flow rates (3 – 7 ml min⁻¹), with the feed being delivered using high pressure
25 N₂ rather than a mechanical pump. The design incorporated the *in-situ* collection of solids through
26 a double tube design. The algae was processed at 5 wt% and the results were compared to those
27 from a batch reactor operated at equivalent conditions. By combining high heating rates with
28 extended reaction times, the continuous system was able to yield significantly enhanced bio-crude
29 yields compared to the batch system. This demonstrates the need for inexpensive continuous
30 processing in the lab, to aid in scale up decision making.

31 **1 Introduction**

32 Hydrothermal liquefaction (HTL) of microalgae represents a promising pathway for the production
33 of sustainable, 3rd generation biofuels [1]. It converts the entire algae, including proteins and
34 carbohydrates as well as lipids, and can therefore use faster growing, and cheaper algae than
35 conventional lipid-based processes [2]. It is conducted at high water loadings, typically ranging
36 from around 80 wt% to 95 wt% [3], significantly reducing the algae drying requirements, and
37 saving up to 90 % of the total energy costs associated with algal harvesting [4]. Finally, HTL allows
38 a significant proportion of the nitrogen and phosphorus initially present in the algae to partition
39 into the water phase, facilitating the recovery and recycling of these valuable resources [5-7].

40 At the same time, HTL reactions require high pressures to maintain water in its liquid phase, and
41 prevent the latent heat losses associated with vaporisation [1]. Based on steam tables, minimum
42 reaction pressures can be calculated to range from 64 bar to 210 bar for typical reaction
43 temperatures of 280 °C to 370 °C [8]. Furthermore, the reaction involves a thick biomass slurry,
44 containing algal particles suspended in an aqueous phase and yields four different product
45 phases (solids, biocrude oil, water and gas), which all need to be collected and separated post
46 reaction. This makes it difficult to carry out this process under continuous flow in a laboratory
47 environment. Consequently, the vast majority of algal HTL research has been conducted within

48 batch reactors. Although batch systems allow the evaluation and comparison of different
49 feedstocks and reaction conditions, they are not directly applicable to large-scale industrial
50 processing, which heavily relies on continuous flow processes with much higher volumetric
51 productivities [9]. Furthermore, batch systems are unable to provide the same level of control as
52 continuous flow systems and struggle to combine high heating rates, which have been shown to
53 be beneficial for higher biocrude yields [10, 11], with extended reaction times, required to achieve
54 full biomass conversion.

55 Only few continuous liquefaction studies have been published to date [12-14], and have often
56 been restricted to low algae loadings due to operational problems with the feed delivery pump
57 [15], or the formation of blockages within the product collection system [16]. An exception is the
58 work by Elliott *et al.*, who managed to process a biomass slurry with an algae loading of 35 wt%
59 [17]. Their design employed a modified dual syringe pump system to push the algae through the
60 system, and pre-heated the algae feed inside a continuous stirred tank reactor (CSTR), before
61 introducing it into a plug flow reactor (PFR) for further conversion. However, this design is
62 expensive, and may therefore restrict its widespread use by the wider research community.

63 Almost all continuous liquefaction experiments described in the literature were conducted in
64 PFRs, with the exception of the work by López Barreiro *et al.*, who employed a CSTR with a
65 reaction temperature of 350 °C and a residence time of 15 minutes [18]. However, using this
66 system, overall bio-crude yields were slightly reduced compared to batch reactions, and this was
67 attributed to the cross-reaction between primary intermediates and final reaction products. In
68 contrast, the results from the PFR systems were generally not compared to equivalent batch data,
69 although both Biller *et al.* [14] and Jazrawi *et al.* [16] reported increased bio-crude yields as the
70 system flowrates were increased.

71 Another challenge with the HTL process is the tight process economics of producing a relatively
72 low value fuel product. Algae cultivation is relatively expensive and nutrient-intensive [19], and

73 consequently cost predictions for the production of algal bio-crude via HTL were found to
74 significantly exceed current transportation fuel market prices [20]. It is therefore unlikely that the
75 fuel product will be able to pay for the entire liquefaction process on its own and additional value
76 streams need to be identified and developed which can help to subsidise the fuel production costs.
77 Potential options include the production of by-products with sufficient market share, such as
78 animal feeds, protein supplements, fertilizers or bio-plastics [1], or combining algae cultivation
79 with secondary functions such as carbon sequestration [21-23] or bioremediation [24]. Particularly
80 the combination of algae biomass production with wastewater treatment has the potential to result
81 in substantial cost savings, as well as significantly reducing the overall environmental impact of
82 the two processes [25]. One of the main objectives of wastewater treatment is the removal of
83 nutrients, particularly phosphorus and nitrogen, which can cause eutrophication. Combining
84 wastewater treatment with algae cultivation significantly reduces the amount of additional
85 nutrients required for algae growth [26]. Global municipal waste water production amounts to
86 approximately 300 billion m³, of which just over 50 % is currently treated [27]. Consequently there
87 is huge potential, particularly in less-developed economies, to apply algae cultivation to improve
88 water quality whilst producing a sustainable fuel by-product.

89 In this investigation the design of a continuous lab-based HTL system is presented, specifically
90 designed to represent an inexpensive alternative to laboratory systems already described in the
91 literature. The system was commissioned and operated using a 5 wt% microalgal slurry produced
92 during the bioremediation of domestic wastewater. During the study the effect of the operating
93 temperature and system flow rate were investigated and compared to the results obtained from a
94 transient batch reactor, operated under equivalent conditions (reaction temperature and heating
95 rates).

96 2 Material and methods

97 2.1 Biomass preparation and analysis

98 The algae used for this project was obtained from a collaboration with the Algae Research Group
99 (Department of Biology and Biochemistry, University of Bath) and a local water company, who
100 cultivated the algae to provide tertiary removal of nitrogen and phosphorus from domestic
101 wastewater. As such, the algae (community of locally sourced *Scenedesmus* and *Chlorella*
102 strains) was specifically selected for its efficiency in phosphate uptake, as well as its ability to
103 settle out quickly to facilitate its recovery following wastewater treatment.

104 After harvesting, the algae were allowed to settle for a number of days, and the excess water was
105 decanted. The aqueous biomass was subsequently centrifuged to obtain an algal slurry with a
106 biomass concentration of 21.7 wt%, which was separated into 50 g batches and stored at around
107 -4 °C.

108 For each experiment, the required amount of algae was defrosted and diluted with D.I. water to
109 obtain the desired experimental concentration of 5 wt%. The exact algae loading was determined
110 by oven-drying aliquots of the well-mixed algae slurry.

111 The algae ash content was determined using thermogravimetric (TGA) analysis of the dried algae,
112 according to literature precedent [28]. The analysis was conducted in air on a Setaram TG-92
113 microbalance, using a ramp rate of 10 °C min⁻¹ to 500 °C, followed by a ramp of 20 °C min⁻¹ to
114 900 °C. This analysis was repeated with the same ramp rate on a TG-DSC-EGA analyser
115 (Setaram Setsys Evolution TGA 16/18, Pfeiffer Vacuum Omnistar GSD 320), to determine the
116 gas phase composition. The energy density of the dried algae was measured on an IKA®
117 Calorimeter C1 analyser, using a 0.5 g sample, and the weight of the combustion residue was
118 recorded, for comparison.

119 The carbohydrate assay was carried out according to Taylor [29], incorporating an upfront two-
120 step hydrolysis protocol adapted from Kostas *et al.* [30]. The lipid content was determined post
121 conversion to fatty acid methyl esters (FAMES) using GC-MS analysis, as described previously
122 [31]. The protein content was estimated using the algal nitrogen content and applying the standard
123 Jones' factor of 6.25 [32].

124 2.2 Batch reactions

125 Batch liquefaction reactions were conducted using the same set-up described in our earlier work
126 [24, 31]. Briefly, it consisted of a 50 mL reactor, fitted with an internal thermocouple and connected
127 to a pressure gauge and vent valve and heated inside a tubular furnace. Each reaction was
128 conducted using approximately 20 g of the pre-mixed algae slurry (5 wt% algae loading). During
129 reactions, the reactor was placed inside the preheated furnace until the desired reaction
130 temperature (300 °C – 340 °C) was reached. At this point, the reactor was immediately removed
131 from the furnace and left to cool in ambient air. Different heating rates (at a constant reaction
132 temperature of 320 °C) ranging from 10.1 °C min⁻¹ to 52.6 °C min⁻¹ were obtained by varying the
133 furnace temperature between 500 °C and 800 °C.

134 Following reactions, the reactor was vented and the reactor contents were decanted through pre-
135 weighted filter paper, to recover the water phase (filtrate). The aqueous residue, defined as the
136 non-volatile material present in the aqueous phase, was determined gravimetrically after removal
137 of the water by overnight drying of the aqueous phase aliquots in a drying oven (> 60°C). The
138 biocrude phase was recovered by rinsing the reactor wall and filter residue with chloroform until
139 the solvent remained clear and evaporating the solvent under vacuum. Solid yields were
140 determined from the mass of retentate collected on the filter paper.

141 All reactions were conducted in triplicate, and the experimental variation was determined in terms
142 of standard deviations.

143 2.3 Continuous reactor design and operation

144 2.3.1 System design

145 The continuous-flow liquefaction system used for this study can be divided into a number of sub-
146 sections: a feed delivery system, the liquefaction reactor itself and a product collection and flow
147 control system (Figure 1). The full P&ID is available in the supporting information.

148 The feed delivery system consisted of two parallel feed reservoirs, pressurised from a high-
149 pressure nitrogen cylinder and connected via a valve manifold. This design allowed each feed
150 reservoir to be isolated in turn, whilst maintaining flow through the other, to enable topping up with
151 algae, or switch-over from water to algae flow and vice versa, without loss of system flow. The
152 system pressure was controlled to between 160 bar and 165 bar using the pressure regulator on
153 the nitrogen cylinder, limiting the maximum reaction temperature to 347 °C.

154 The reactor consisted of a vertical, double tube design, heated inside a tubular furnace. Cold
155 algae feed entered through the inner tube from the top, where it started to be heated, the products
156 then flowed back up the annulus of the reactor and exited the reactor from the top. This design
157 was chosen to allow fast heating of the algae and collection of the solid products at the bottom of
158 the reactor, preventing their accumulation within the flow line, which would lead to reactor
159 blockages. These solids could then be removed at the end of the reaction. The reaction
160 temperature was determined using a thermocouple (T1) located at the outlet of the inner tube,
161 and a second thermocouple (T2) at the reactor outlet was used to estimate the temperature
162 gradient throughout the reactor.

163 Batch-wise collection of the liquid reaction products at pressure and elevated temperatures was
164 conducted within two parallel, nitrogen-filled collection pots, similar to the configuration previously
165 employed by Elliott *et al.* [17]. The system flow was controlled indirectly by regulating the flow of
166 nitrogen and reaction gases from the liquid collection pots to a vent line, using a manual gas flow

167 meter. To protect the flowmeter against overpressure, a pressure-reducing regulator was installed
168 upstream to reduce the pressure below 10 bar. Once one of the pots was full, flow was redirected
169 to the other, and the pot was vented and drained to recover the liquid reaction products.
170 Subsequently, the pot was re-pressured with nitrogen from a separate gas cylinder, and equalized
171 to the system inlet pressure. Following each liquid recovery step, the collected liquid volume and
172 collection time were recorded to monitor and calibrate the system flow rate.

173 2.3.2 *System operation*

174 Prior to each reaction run, the system was started up on distilled water and the gas flow from the
175 outlet was adjusted to achieve liquid flow rates ranging from 3 mL min⁻¹ to 7 mL min⁻¹. Next, the
176 furnace temperature was increased gradually until the desired reaction temperature (300 –
177 340 °C) was obtained, as measured by T1, the thermocouple located at the bottom of the inner
178 reaction tube. Once steady state was reached, the reaction was started by switching system flow
179 from distilled water to the pre-mixed algae slurry. After flowing a total of 1 L of a 5 wt% algae
180 slurry, the system was maintained at reaction conditions, whilst being purged with distilled water
181 for another two hours, until the liquid at the system outlet started to run clear. At this point, the
182 furnace was turned off and water flow was maintained until the system temperature reduced to a
183 safe level, at which point it was isolated and allowed to cool overnight. Depending on the system
184 flow rate, the liquid collection pots were drained every 15 to 30 minutes, to prevent overflow of
185 the reaction liquids into the gas lines. The total collected liquid volume was recorded to determine
186 the remaining feed volume, and prevent the system from running dry.

187 A repeat run at the medium reaction temperature of 320 °C and flowrate of 5 mL min⁻¹ was used
188 to estimate the experimental variation of the system.

189 2.3.3 *Product recovery*

190 Neither the gas yield nor the composition was investigated as the study focused on liquid phase
191 and solid products. Bio-crude and water products recovered from the liquid collection pots were
192 collected and separated using vacuum filtration through pre-weighed filter paper. After each
193 collection interval, a 20 mL aliquot of reaction water was re-filtered by gravity, to ensure full
194 removal of any entrained solids, and retained for further analysis. Any remaining water was re-
195 filtered under vacuum and combined into two separate samples: water collected during algae flow
196 and water collected post reaction, during water purging. The bio-crude product was recovered by
197 washing all filter papers with chloroform and combined into a single fraction. Solid carry-over to
198 the outlet was determined by re-weighing the dried filter papers following bio-crude removal.

199 At the end of each reaction run, the system was fully dismantled to allow the recovery of solids
200 and bio-crude product residue from the reactor and the system pipework. The reactor contents
201 were filtered and thoroughly washed with water and chloroform to obtain the solid products and a
202 heavy bio-crude fraction, labelled 'heavy bio-crude'. Chloroform washing of the reactor outlet
203 piping and collection pots allowed the recovery of 'pipe bio-crude ', which was eventually
204 combined with the bio-crude product from the system outlet to form the 'light bio-crude' fraction.

205 Product yields were calculated on a dry biomass basis, without further correction for the ash
206 content.

207 2.4 *Product analysis*

208 Elemental (CHN) analysis of the bio-crude samples was carried out externally on a Carlo Erba
209 Flash 2000 Elemental Analyser. For the continuous reactions, the light and heavy bio-crude
210 fractions were analysed separately, before calculating weighted averages to determine the
211 elemental distribution to the total biocrude phase. In the case of the batch reactions, only the most

212 representative of the three repeats (yield closest to average) was analysed for each reaction
213 condition.

214 The water content of the combined bio-crude from all continuous HTL reactions was determined
215 by Karl Fischer titration. Prior to analysis, the sample was diluted in chloroform to 2 wt%, and
216 calibrated against the chloroform water content. The energy density of the combined bio-crude
217 was measured on an IKA® Calorimeter C1 analyser, using a 0.5 g sample. This analysis was also
218 used to estimate the ash content of the bio-crude and verified against the results from TGA.

219 The concentration of ammonium ions in the water phase was determined using a Randox Urea
220 analysis test kit. Prior to analysis, the samples were diluted with D.I. water to a concentration of
221 20 vol%. Subsequently 10 µL of sample was reacted for 5 min with 1000 µL of a urease reactant,
222 followed by the addition of 200 µL of sodium hypochlorite solution to induce the colour change.
223 Finally, the sample absorbance was measured at 600 nm and calibrated using a reagent blank
224 and standard solution.

225 Total organic carbon (TOC), total inorganic carbon (IC) and total nitrogen (TN) of the water phase
226 products were determined on a Shimadzu Corp. total organic carbon analyser (TOC-L), linked to
227 a total nitrogen analyser (TNM-L) and autosampler (ASI-L). Prior to analysis, samples were
228 diluted with D.I. water to 12.5 vol%. For the continuous reactions, the total carbon and nitrogen
229 recovery to the water phase was estimated using the carbon and nitrogen concentrations in the
230 combined water phase obtained during the entire reaction period.

231 **3 Results and discussion**

232 **3.1 Biomass characterization**

233 Thermogravimetric analysis (TGA) of the dried algae resulted in a total weight loss of 79.2 wt%,
234 associated with the loss of residual moisture (5.0 wt%), two exothermic peaks at temperatures of

235 350 °C and 545 °C (65.1 wt%) and an endothermic peak at 831 °C (9.1 wt%, supporting
236 information). The two exothermic peaks can be associated with the combustion of organic
237 biomass components, confirmed by the detection of both carbon dioxide and water during TG-
238 MS analysis, whereas the only gas released over the high-temperature endothermic peak was
239 carbon dioxide. Therefore it is likely that this peak was associated with the thermal decomposition
240 of carbonates, as previously detected during TGA analysis of macroalgae [33], and suggests that
241 the wastewater derived algae sequestered atmospheric carbon in both organic and inorganic
242 form. As the ash content is generally defined as the inorganic biomass fraction, it was calculated
243 to include these carbonates by using the residual sample weight at 650 °C. The resulting value of
244 29.9 wt% compares to a residue weight of only 20.8 wt% at 900 °C and a combustion residue of
245 30.1 % using bomb calorimetry.

246 Biochemical compositional analysis of the algae showed that it was predominantly composed of
247 proteins, and contained only low amounts of lipids and carbohydrates (Table 1). Overall, the
248 contribution of these three major biochemical compounds was 59.1wt%, with an ash content of
249 29.9 wt%., resulting in an energy density of 12.72 MJ kg⁻¹.

250 3.2 System design

251 The system was specifically designed to provide a lower-cost alternative to the HTL systems
252 already used in the literature. During the commissioning process, a number of operational
253 challenges were encountered, which required significant modifications to the initial design, to
254 allow the processing of the entire biomass inventory. Particular challenges were the formation of
255 blockages within the reactor tube itself, and large fluctuations in system flow and temperature, as
256 a result of control valve blockages. In this section, the final design is discussed and compared to
257 alternative systems in the literature.

258 3.2.1 Flow delivery

259 To date, most continuous HTL systems described in the literature have employed high-pressure
260 mechanical pumps to push the algae feed through the system. However, even though mechanical
261 pumps are the expected method of choice for larger-scale operation, laboratory-scale pumps, that
262 can generate the high required reaction pressure as well as being able to handle the semi-solid
263 algal particles in the feed, (such as the modified dual syringe pump system used by Elliott *et al.*
264 [17]) are expensive, and still not directly applicable to industrial processing. Alternative pumps
265 used in the literature have either exceeded the desired laboratory-scale flow rates, such as the
266 triplex piston pump system used by Jazrawi *et al.* [16] and Cole *et al.* [12] (15-90 L h⁻¹) or have
267 struggled to process elevated biomass concentrations, such as the HPLC pump used by Patel
268 and Hellgardt [15].

269 In contrast, by using high-pressure nitrogen as the algae driving force, our design eliminates the
270 requirement of a mechanical pump completely, and thereby reduces the risk of blockages within
271 the pump cavities as well as representing a lower-cost lab scale alternative to existing HTL
272 systems. It provides a high degree of flexibility, both in terms of flow rate and feed pressure, and
273 the double feed cylinder arrangement allows continuous feeding of algae. Despite initial concerns
274 of nitrogen break-through, resulting in flow fluctuations, the final design was found to be able to
275 deliver a constant liquid flowrate throughout the entire reaction period, as determined from the
276 liquid accumulation within the liquid collection pots, as well as constant reaction temperatures
277 (supplementary information).

278 A disadvantage is the lack of the precise metering functionality of some of the mechanical pumps,
279 and consequently the system flow rate had to be controlled separately. Furthermore, as nitrogen
280 is a compressible fluid, variations in the pressure drop through the system could have a larger
281 effect on the algae flow rate through the system. This problem was mitigated by controlling the
282 product flow from the outlet instead.

283 3.2.2 Reactor configuration

284 Consistent with the majority of continuous HTL systems described in the literature, our design
285 employed a modified PFR to conduct the liquefaction reaction. However, to the best of our
286 knowledge this is the first time a double-tube design to allow the collection of the solid reaction
287 products within the reactor itself has been applied to this reaction. The main reason for adapting
288 this arrangement was to address operational problems caused by the extensive formation of
289 blockages within a single-pass, up-flow reactor. These blockages were predominantly attributed
290 to the accumulation of solid products within the reactor tube, possibly as a result of insufficient
291 flow velocities through the system to allow full fluidisation of this phase.

292 No previous publication reported significant issues with blockages formed within the reactor,
293 however it should be noted that in many cases the algae loadings were significantly lower than in
294 the present work [13, 15, 34], or the authors employed a co-solvent to prevent plugging issues in
295 the first place [12, 15]. An exception is the work by Elliott *et al.*, who processed a feed with an
296 algae concentration of up to 35 wt%, however this group employed a CSTR to pre-heat the algae
297 feed from 133 °C to the final reaction temperature before allowing the reaction to be completed
298 in a PFR [17]. It should also be noted that the algal biomass used in most previous HTL reactions
299 was less challenging to process than the wastewater algae used in this project, which contained
300 a very high ash content (~ 30 %), allowing the algae to settle out quickly following wastewater
301 treatment. This high ash content may have contributed to the severity of the reactor blockages
302 experienced with our initial design.

303 An additional benefit of the double-tube reactor is that it combines very fast heating rates with
304 extended reaction times, and reduces the presence of hot-spots at the reactor wall, which might
305 catalyse the formation of radicals, which in turn could initiate polymerisation reactions. Based on
306 the range of system flow rates (3 mL min⁻¹ to 7 mL min⁻¹), heating rates were estimated to have
307 ranged from 28.8 °C min⁻¹ to 67.6 °C min⁻¹, whilst the residence time of the hot reagents/products

308 in the outer tube varied between 17.7 and 41.8 minutes. The design also allowed the partial heat
309 recovery from the hot reaction product in the reactor, without causing the plugging problems
310 reported by Elliott *et al.* when pre-heating a lignocellulosic reaction feed above 133 °C [17]. At the
311 same time, temperature drops between 45 °C and 58 °C were recorded between the bottom of
312 the inner tube and the outlet of the reactor.

313 The solid retention within the reactor exceeded 95 % for all reactions, with little correlation to the
314 selected reaction conditions (temperature and flow). This suggests that gravity settling was highly
315 effective in the recovery of this solid fraction. Even so, the solid capacity of the reactor is limited,
316 and therefore in future designs it may be necessary to incorporate a solid removal system to allow
317 extended system operation.

318 3.2.3 *Product collection and flow control*

319 Prior to designing the liquid collection system, consisting of two parallel, nitrogen-filled collection
320 pots, an attempt was made to control the system flow directly, using a liquid flowmeter at the
321 system outlet. However, the high viscosity of the biocrude at room temperature resulted in the
322 clogging of the control valves, causing significant fluctuations of the system flow. Similar problems
323 were previously reported by Jazrawi *et al.*, who experienced significant pressure fluctuations as
324 a result of transient blockages of their back-pressure control valve [16]. In contrast, controlling the
325 system backpressure on the outflow of gas avoided the requirement of having to pass the viscous
326 biocrude through the restrictions within a control valve. Although this design required the batch-
327 wise removal of liquid products, followed by repressurisation of the collection pots, further
328 modifications to install a level controller within the collection pot would allow the continuous
329 recovery of the liquid products. Furthermore, flow control could be improved by installing a liquid
330 flowmeter to set the operating variable of an automatic control valve at the gas outlet.

331 3.2.4 System operation

332 During the operation of the system, depending on the reaction temperature and the system flow
333 rate of any particular experiment, the collection pot temperature varied from 56.3 °C to 125.9 °C,
334 as a result of different residence times, and therefore different heat losses to the environment.
335 The percentage of the total recovered bio-crude fraction collected from the outlet was found to be
336 directly proportional to this temperature, whereas the opposite trend was observed for the bio-
337 crude obtained from the reactor outlet piping, post reaction (supplementary information). These
338 trends could be related to increases in the biocrude viscosity and reduced miscibility with the
339 water phase, as the collection temperature is reduced. However, all reactions were conducted
340 with the same amount of algae, and consequently, it is not known whether bio-crude accumulation
341 within the system pipework remained constant over the entire reaction period, or whether it
342 reached a saturation point, after which all additional bio-crude exited from the system. Continuous
343 bio-crude accumulation would eventually result in the formation of system blockages, and
344 therefore system operation should be investigated over longer reaction periods. As the partitioning
345 between bio-crude remaining in the system pipework and bio-crude recovered from the outlet
346 appeared to depend mostly on the collection temperature, these two fractions were combined into
347 a single 'light-biocrude' phase.

348 In contrast, the fraction of bio-crude recovered from the reactor was found to be independent of
349 the collection temperatures. As this bio-crude cannot be easily recovered from the system during
350 continuous flow and was found to be much more viscous than the biocrude fractions recovered
351 from the outlet and the reactor pipework, which suggests a different chemical composition, it was
352 kept as a separate, 'heavy bio-crude' phase, further GC-MS analysis confirmed the different
353 chemical nature of both bio-crude samples (see supporting information).

354 Using our system, it was possible to consistently process 1 L of a 5 wt% algae slurry, whilst
355 maintaining constant reaction temperatures and system flow rates. Whilst the system required a

356 lot of operator input, it represents a significantly lower cost alternative to the systems already used
357 in the literature, making it feasible as a bench-scale laboratory system.

358 3.3 Batch conversion

359 Prior to converting the wastewater-derived algae within the continuous HTL system, a number of
360 baseline reactions were conducted in a batch system to determine the effect of reaction
361 temperature and heating rate on the resulting product distribution. Batch reactions were
362 conducted under transient conditions, which means that the reactors were removed from the
363 furnace as soon as the desired reaction temperature was reached, giving an effective reaction
364 time of 0 minutes. This approach allows much faster heating rates than the more commonly used
365 isothermal systems, where the reaction temperature is maintained for a prolonged period of time.

366 3.3.1 *Effect of reaction temperature*

367 The conversion of the wastewater-derived algae was studied at three different temperatures
368 (303 °C, 322 °C and 339 °C) with a constant furnace temperature of 700 °C, resulting in averaged
369 heating rates ranging from 33.8 °C min⁻¹ at 339 °C to 37.6 °C min⁻¹ at 303 °C. As the reaction
370 temperature was increased from 303 °C to 339 °C, solid yields were found to reduce from
371 43.6 wt% to 38.2 wt% (Figure 2a). This is consistent with our earlier work [31] and can be
372 associated with an increase in algae conversion resulting in reduced solid retention of the organic
373 biomass components. As the reaction temperature was increased from 303 °C to 321 °C, the
374 water phase residue yield also experienced a remarkable decrease from 29.9 wt% to 20.7 wt%,
375 which could be partially attributed to the simultaneous increase in biocrude yield (12.1 wt% to
376 17.1 wt%) and a reduction in the overall mass balance closure from 85.5 % to 79.2 %. The
377 unaccounted product fraction can be assigned to gaseous products, as well as volatile organic
378 reaction products present in the aqueous phase, which are lost during the drying of the water
379 phase residue. As the reaction temperature was increased further to 339 °C, the water residue

380 yield increased by 3.3 wt%, closely matching the simultaneous reduction in solid yields (41.5 wt%
381 to 38.2 wt%), although a slight decrease in bio-crude yield (17.1 wt% to 15.9 wt%) was also
382 experienced over the same temperature range.

383 The highest carbon (30.2 %) and hydrogen (27.6 %) recoveries to the biocrude were achieved at
384 the medium reaction temperature, producing a combined bio-crude (heavy + light) with a nitrogen
385 content of 4.0 wt%, lower than the biocrudes obtained at the other two reaction temperatures
386 (Figure 2b). Consistent with the low overall bio-crude yield, the carbon and hydrogen recoveries
387 obtained at 303 °C were much lower, although the difference in nitrogen recovery was much
388 smaller, indicating that a large proportion of nitrogen-containing compounds was already
389 incorporated into the biocrude at low reaction temperatures.

390 However, when increasing the reaction temperature from 322 °C to 339 °C, the hydrogen and
391 carbon distribution to the bio-crude reduced, whereas the nitrogen retention increased,
392 suggesting that nitrogen containing compounds continued to be converted into biocrude
393 components at all reaction temperatures. These findings are consistent with previous studies [11,
394 16, 35] and suggest that significantly increasing the reaction temperatures above 320 °C had no
395 beneficial impact on the biocrude recovery.

396 Contrary to trends for the biocrude, the carbon and nitrogen recoveries to the water phase
397 reduced with increasing reaction temperatures (Figure 2c). Whilst the maximum combined carbon
398 recovery to the water and bio-crude phases of 59.9 % was still obtained at 322 °C, the combined
399 nitrogen recovery decreased from 77.5 % to 75.5 % as the reaction temperature was raised from
400 303 °C to 339 °C. A potential explanation for these trends is that the majority of nitrogen
401 partitioned from the solid phase to the other phases at the lowest reaction temperature, whereas
402 carbon transfer from the solid to the aqueous and bio-crude phases continued up to a temperature
403 of 322 °C, beyond which carbon started to be lost to the gas phase. It can also be noted, that the

404 total nitrogen content in the aqueous phase is a very good match to the ammonium ion content,
405 indicating that very few organic nitrogen compounds were present.

406 3.3.2 *Effect of heating rate*

407 Four different heating rates, ranging from 10.1 °C.min⁻¹ to 52.6 °C.min⁻¹ were obtained by varying
408 the furnace temperature between 500 °C and 800 °C. It should be noted that these heating rates
409 represent average, rather than absolute values, as they dropped off as the reaction temperature
410 was approached, particularly for the lower furnace temperatures. All reactions were conducted to
411 a maximum reaction temperature of 320 °C.

412 At the two lower heating rates, the solid yields remained approximately constant around 40 wt%,
413 but increased slightly to 41.5 wt% and 42.8 wt% as the heating rates were increased to 35.2 and
414 52.6 °C min⁻¹, respectively (Figure 3a). Bio-crude yields, in turn, increased almost linearly from
415 14.9 wt% to 17.1 wt% as the heating rates were raised from 10.1 °C min⁻¹ to 35.2 °C min⁻¹, but
416 dropped off to 13.5 wt% at the highest heating rate of 52.6 °C min⁻¹. The water residue yields
417 showed the opposite trend to bio-crude yields, decreasing from 24.7 wt% at the lowest heating
418 rate to 20.7 wt% at 35.2 °C min⁻¹, before increasing to 27.7 wt% at the highest heating rate.

419 The increase in solid yields at the higher heating rates can be explained by the reduced reaction
420 time, resulting in the incomplete conversion of the organic biomass components. Bio-crude and
421 residue yields, in turn, appeared to be closely related. As heating rates increased from
422 10.1 °C min⁻¹ to 35.2 °C.min⁻¹, the product distribution shifted from water phase residue towards
423 bio-crude, but at the highest heating rate, the bio-crude yields were at their lowest, whilst
424 maximum water phase residue yields were obtained.

425 The general trend of increasing bio-crude yields with increasing heating rates is consistent with
426 previous results by Faeth *et al.* [10], and Garcia Alba *et al.* [11]. Where the maximum bio-crude
427 yields obtained at the highest heating rate, were significantly higher than optimized bio-crude

428 yields at lower sandbath temperatures [10]. A subsequent publication by the same authors [36]
429 reported that biocrude yields increased when the total reactor loading was reduced from 60 vol%
430 to 10 vol%. These differences were explained by an increase in the apparent biomass
431 concentration, as the same quantity of water needed to evaporate to generate the reaction
432 pressure. An alternative explanation is that the reactions became kinetically and heat-transfer
433 limited as the reaction volume was increased. This could also explain the sharp drop in biocrude
434 yields at the highest heating rate observed in the present study and suggests that the reaction
435 time was potentially too short to achieve full conversion of the water phase residue phase into
436 biocrude components.

437 As expected from the bio-crude yields, the highest carbon and hydrogen retentions were obtained
438 at the heating rate of $35.2\text{ }^{\circ}\text{C min}^{-1}$ (Figure 3b). The reduction in carbon, hydrogen and nitrogen
439 retentions at lower heating rates can be attributed mostly to the reduction in bio-crude yields,
440 whilst the overall bio-crude composition remained relatively constant. In contrast, the bio-crude
441 obtained at the highest heating rate had a noticeably higher nitrogen content of 4.8 wt% than the
442 bio-crude obtained at a heating rate of $35.2\text{ }^{\circ}\text{C min}^{-1}$ (4.0 wt%). This is similar to the results
443 obtained at the lowest reaction temperature and suggests that nitrogen containing compounds
444 preferentially partition to the biocrude under less severe reaction conditions. It is also possible
445 that some of this nitrogen is removed via denitrogenation reactions at higher reaction
446 temperatures, or longer residence times, counteracting the further transfer of nitrogen containing
447 components from the aqueous to the biocrude phase [37].

448 Carbon recoveries to the aqueous phase reduced from 31.9 % to 29.7 % as the heating rate was
449 reduced from $52.6\text{ }^{\circ}\text{C min}^{-1}$ to $35.2\text{ }^{\circ}\text{C min}^{-1}$ (Figure 3c) and reduced further to 27.3 % for a
450 heating rate of $21.8\text{ }^{\circ}\text{C min}^{-1}$. The highest combined carbon recovery to the aqueous and bio-
451 crude phases of 59.9 % was therefore obtained at the heating rate of $35.2\text{ }^{\circ}\text{C min}^{-1}$, compared to
452 recoveries of less than 55.6 % at all other heating rates. This indicates incomplete carbon transfer

453 from the solid to the aqueous and bio-crude phases at very high heating rates, whilst increased
454 reaction times increased the transfer of carbon to the gas phase. In contrast, both the nitrogen
455 recovery to the aqueous phase alone (69.4 % to 61.4 %) and combined nitrogen recovery to the
456 aqueous and bio-crude phases (80.0 % to 71.9 %) reduced steadily as the heating rates were
457 reduced from 52.6 °C min⁻¹ to 10.1 °C min⁻¹. Once again, the nitrogen content in the water phase
458 could be almost exclusively assigned to ammonium ions.

459 3.3.2.1 *Reaction mechanism*

460 The trends in water phase residue and biocrude yields suggest that the two product phases are
461 closely related. Low reaction temperatures and very high heating rates appeared to favour the
462 formation of molecules that partition into the aqueous phase, which were further converted into
463 biocrude as the reaction severity is increased [38]. At the same time, some of the nitrogen
464 incorporated into the biocrude at low temperatures and high heating rates were removed via
465 denitrogenation, reducing the nitrogen content of the bio-crude phase, and the aqueous phases,
466 and resulting in the formation of more volatile reaction products, which were not recovered.

467 The results suggest a stepwise reaction mechanism; first the algae is broken up into water soluble
468 compounds, which then further react to form the biocrude and more volatile reaction products.
469 This is consistent with the previously suggested Maillard type reaction pathways, where
470 carbohydrates and proteins in the biomass are first decomposed into sugars and amino acids,
471 which then further react via dehydration reactions to form heavier, water-insoluble compounds
472 [39, 40].

473 However, the algae decomposition into intermediates and their subsequent reactions to form bio-
474 crude, water phase and gaseous products, can follow many different pathways and the ultimate
475 product distribution depends on the relative reaction kinetics between these pathways. Low
476 heating rates would therefore favour reactions with lower activation energies, consuming a
477 significant proportion of the reaction intermediates before the temperature rises to a level where

478 higher energy reactions can occur. Based on the trends observed for biocrude yields and heating
479 rate, the reactions resulting in the formation of biocrude appear to have higher activation energies
480 than the reactions resulting in the formation of alternative product phases.

481 However, at the highest heating rates, the reaction time appears to be insufficient to allow full
482 conversion of the biomass or the reaction intermediates, resulting in a sharp drop in biocrude
483 yields. Unfortunately, the transient batch reactors used in this study did not allow the combination
484 of high heating rates with extended reaction times, potentially limiting the maximum biocrude yield
485 that could be obtained. Consequently, the continuous system, which combines higher heating
486 rates with extended reaction times, was expected to provide more favourable product
487 distributions.

488 3.4 Continuous conversion

489 The continuous reaction system was operated at four different temperatures (302 °C, 320 °C,
490 328 °C and 344 °C) and three different flow rates (3 mL min⁻¹, 5 mL min⁻¹ and 7 mL min⁻¹). These
491 conditions corresponded to heating rates ranging from 28.8 °C min⁻¹ to 67.6 °C min⁻¹, comparable
492 to the heating rates achieved with the batch system (10.1 °C.min⁻¹ to 52.6 °C.min⁻¹). water

493 3.4.1 *Effect of reaction temperature*

494 The effect of the reaction temperatures on the product distribution was studied at a constant
495 system feed flow rate of 7 mL min⁻¹ (Figure 4a). Consistent with the findings from the batch study,
496 solid yields were generally lower at higher reaction temperatures, although there was a high
497 degree of experimental uncertainty, related to the difficulty of fully recovering the solid phase from
498 the bottom of the reactor. Water phase residue yields followed a clearer trend, decreasing steadily
499 from 19.8 wt% at 302 °C to 13.4 wt% at 344 °C. The trends in biocrude yields appeared to be
500 more complex. Whilst the maximum heavy bio-crude yields (5.8 wt%) were obtained at the lowest
501 reaction temperature of 302 °C, they decreased to a minimum of 3.5 wt% at 320 °C, before

502 recovering to 4.5 wt% and 5.2 wt% at reaction temperatures of 328 °C and 344 °C, respectively.
503 Light bio-crude yields were lowest at the minimum reaction temperature of 302 °C (14.3 wt%),
504 and remained approximately constant around 15 wt% to 16 wt% for the other three reaction
505 temperatures.

506 The initial reduction in the heavy bio-crude yields from 5.8 wt% to 3.5 wt%, as the reaction
507 temperatures were increased from 302 °C to 320 °C, closely matches the simultaneous increase
508 in light bio-crude yields from 14.3 wt% to 16.0 wt%. This could be the result of increased cracking
509 reactions of heavy bio-crude components to form lighter, less viscous compounds, which were
510 carried over into the light bio-crude phase. Conversely, the subsequent increase in heavy bio-
511 crude yields at higher reaction temperatures could be caused by the volatilisation of heavy
512 organics bound to the solid phase product.

513 Based on the continuous conversion results and contrary to the batch study, the aqueous phase
514 residue yields appeared to show little correlation to the biocrude yields. Instead the decrease in
515 this phase could be mostly attributed to a decrease in overall recovered product from 69.5 wt%
516 to 63.0 wt%, suggesting the formation of more volatile reaction products at higher reaction
517 temperatures, partitioning into the gas phase, or lost during the recovery of the water phase
518 residue. However, it is possible that these volatile products were formed from the bio-crude phase
519 instead, as a result of gasification, denitrogenation and deoxygenation reactions, counteracting
520 the additional conversion of the water-phase residue into the light bio-crude product phase. It
521 should also be noted that, contrary to the batch study, bio-crude yields did not reduce at higher
522 reaction temperatures, which could indeed suggest further conversion of the water phase residue
523 into the light bio-crude phase.

524 To investigate this in more detail, the carbon, hydrogen and nitrogen balance to the bio-crude
525 phase was calculated from the elemental analysis of the two biocrude fractions (Figure 4b).
526 Increasing the reaction temperature from 302 °C to 320 °C resulted in a significant increase in

527 carbon retention from 35.0 % to 40.8 %, but at higher temperatures the carbon retention remained
528 approximately constant. Nitrogen retentions reduced steadily from 16.3 % at 302 °C to 11.7 % at
529 344 °C, which is opposite to the trend observed during the batch experiments. This could suggest
530 that the extended residence time in the continuous flow reactor allowed more denitrogenation
531 reactions to take place. Finally, the hydrogen retention was highest at 320 °C and dropped sharply
532 as the reaction temperature was increased further. This could be explained by the participation of
533 hydrogen in the denitrogenation pathway to form ammonia and is consistent with the steady
534 increase in the yield of ammonia in the water phase from 1.7 wt% to 3.0 wt%, corresponding to a
535 nitrogen recovery of 23.2 % and 41.1 %, respectively, as the reaction temperature was raised
536 from 302 °C to 344 °C (Supplementary information).

537 The carbon recovery to the water phase steadily decreased from 34.8 % to 26.8 % as the reaction
538 temperature was increased from 302 °C to 328 °C, consisting almost exclusively of organic
539 carbon, resulting in a combined carbon recovery to the bio-crude and water phases of 71.6 % to
540 64.5 %. Presumably, the remaining carbon was distributed between the solid phase, containing
541 most of the inorganic carbon in the algae (~ 10 wt%) and the gas phase (CO₂). The nitrogen
542 recovery to the water phase ranged from 87.5% at 302 °C to 73.2 % at 328 °C, before recovering
543 to 82.1 % at the highest reaction temperature, corresponding to combined nitrogen recoveries
544 between 103.8 % and 86.7 %. These high mass balance closures suggest very little nitrogen
545 distribution to the solid or gas phases.

546 *3.4.2 Effect of system flow rate*

547 To study the effect of the system flow rate on the product distribution, the reaction temperature
548 was kept constant at 320 °C (Figure 5a). Increasing the flow rate from 3.0 mL min⁻¹ to 6.9 mL min⁻¹
549 resulted in a clear increase in solid yields from 27.7 wt% to 35.2 wt%. This is consistent with the
550 results from the batch study, where higher heating rates were found to produce more solid,
551 probably as a result of reduced reaction times. However, the solid yields from the continuous

552 system (maximum of 35.2 wt%) were much lower than those from the batch reactor (minimum of
553 39.7 wt%), and at the lowest flow rate approached the value of the initial algae ash content,
554 suggesting full conversion of the organic biomass fraction. This is unsurprising, as even at the
555 fastest flow rate, the reaction time in the continuous system (17.8 min) significantly exceeded the
556 reaction times obtained within the batch system. Furthermore, the solid products remained in the
557 bottom of the reactor for a period of several hours, allowing the reaction to proceed even after the
558 algal flow was stopped. Consequently, the increase in solid yields at higher system flows cannot
559 be solely attributed to differences in reaction times, but may instead be related to the heating
560 rates. It should also be noted that the reaction temperature was recorded by T1 at the bottom of
561 the inner tube, whereas the temperatures at the bottom of the reactor could have been higher,
562 particularly for the less turbulent, lower system flow rates, which could have further impacted on
563 the organic solids conversion.

564 Like the solid yields, the water phase residue yields obtained from the continuous reactor
565 (13.8 wt% to 20.9 wt%) were significantly lower than those obtained from the batch study
566 (20.7 wt% to 27.7 wt%) but in this instance, the residue yields increased with increasing system
567 flow rate, whereas in the batch study they generally reduced as the heating rates were increased.
568 Even more complex trends were obtained for the bio-crude yields. The highest amount of 'light
569 bio-crude' was obtained at the highest flow rate of 6.9 mL min⁻¹ (17.6 wt%), dropped to a minimum
570 of 13.9 wt% at 5.0 mL min⁻¹, and then increased to 15.4 wt% at the lowest system flow rate. The
571 'heavy bio-crude' yields followed a different trend, reaching a maximum of 4.9 wt% at 3.0 mL min⁻¹
572 ¹, a minimum of 3.6 wt% at 5.0 mL min⁻¹ and 4.3 wt% at 6.9 mL min⁻¹.

573 A potential explanation for these trends is the contribution of both fast, competitive reactions,
574 favoured by high heating rates, as well as slower reactions, enhanced at higher residence times,
575 to the overall bio-crude formation. The medium flow rate of 5.0 mL min⁻¹ was too slow to realise
576 the benefit of high heating rates, whilst the reactor residence time was too short to allow full

577 conversion of the components in the aqueous phase into the biocrude phase. Slower heating
578 rates and longer reaction times may also have favoured the occurrence of polymerisation
579 reactions, resulting in the formation of heavier bio-crude components, potentially containing
580 greater amounts of aromatics and heteroatoms.

581 This is consistent with the elemental distributions to the biocrude phase obtained for the three
582 system flow rates (Figure 5b). The bio-crude formed at 3.0 mL min^{-1} contained a lower hydrogen
583 and a higher nitrogen content than the bio-crude phases formed at the higher system flow rates.
584 Even though the carbon recovery of 37.8 % was higher than at the medium flow rate, it was still
585 lower than the carbon recovery at 6.9 mL min^{-1} (40.8 %). Together with a much higher hydrogen,
586 and lower nitrogen recovery, the best results, both in terms of bio-crude yields and quality, were
587 obtained at the highest system flow rate. However, it is interesting to note that the heavy bio-
588 crude contained a higher carbon and hydrogen and lower nitrogen content than the light bio-crude
589 (Supplementary information).

590 The carbon retention to the water phase followed a similar trend to the retention in the biocrude,
591 reaching a maximum of 30.8 % at a flowrate of 6.9 mL min^{-1} and a minimum of 26.2 % at the
592 medium flowrate, resulting in total carbon recoveries to the water and bio-crude phases between
593 58.6 % and 71.6 %. The nitrogen recovery to the water phase was also highest at the highest
594 system flowrate (86.7 %) resulting in an overall nitrogen recovery of 101.1 %.

595 For the highest system flow rate, even the yields of light bio-crude on their own (17.6 wt%),
596 exceeded the total bio-crude yields obtained from the batch reactor, which demonstrates the
597 advantage of continuous over batch processing. Therefore, research on continuous flow reactors
598 not only provides results which are much more applicable to large-scale industrial processing, but
599 also has the potential to yield improved biocrude yields and product compositions.

600 Further analysis of the combined light bio-crude phase from all continuous reactions revealed a
601 water content of 0.58 %, an ash content of 2.3 wt% and an energy density of 34.9 MJ kg^{-1} .

602 4 Conclusions

603 Current research on the HTL of microalgae has been mostly restricted to batch reactors due to
604 their lower cost and easier processing, compared to continuous systems. By substituting the high-
605 pressure mechanical pumps used in previous continuous HTL studies with a nitrogen-driven feed
606 delivery system, it was possible to design a lower-cost continuous system, allowing more
607 industrially representative research, compared to the batch reactors commonly used on the lab
608 scale. Data from the continuous monitoring of the system temperature profiles together with
609 constant liquid collection volumes confirmed that the system was able to deliver a constant flow
610 of liquid through the system, with no evidence for gas-breakthrough. In order to prevent the
611 formation of blockages within the reactor, our design incorporated the *in-situ* collection of the solid
612 reaction product by adapting a double-tube design, which also helped to deliver much higher
613 heating rates, whilst providing extended reaction times. Due to the high viscosity of the biocrude
614 at ambient conditions, it was necessary to collect the liquid product phases at elevated
615 temperatures and pressures and control the system flow rate indirectly, using the outflow of
616 nitrogen and reaction gases from the product collection pots. Using this system it was possible to
617 consistently process 1 L of a 5 wt% wastewater-derived algae slurry.

618 Results from the batch study confirmed previous work in the literature, which suggested that
619 increased heating rates could help to improve biocrude yields. This was attributed to the
620 conversion of unstable aqueous phase intermediates during the heating process to form
621 undesired solid or gaseous by-products, before sufficient reaction temperatures were reached to
622 start the bio-crude formation process. Nevertheless, at very high heating rates, biocrude yields
623 reduced sharply and this was ascribed to very short reaction times, insufficient to achieve full
624 biomass conversion.

625 These limitations were not present within the continuous reaction system, which combined fast
626 heating rates with extended reaction times. Consequently, this system was able to produce much

627 higher biocrude yields and lower solid and water phase residue yields than the batch system.
628 Consistent with previous literature findings, the best results were obtained at the highest system
629 flow rate, although the results suggested a competitive effect on bio-crude formation between fast
630 reactions, favoured by high heating rates, and slower reactions, enhanced at higher reactor
631 residence times.

632 Although maximum overall bio-crude yields of 21.9 wt% in this study were relatively low, this can
633 be ascribed to a very high algal ash content of 29.9 wt%, together with a low lipid fraction of
634 7.9 wt%. Given the low cost of this feedstock, the combination of algal wastewater treatment with
635 fuel production via HTL represents a promising economic process, which warrants further
636 investigation.

637

638 **Acknowledgements**

639 This work was funded by the Engineering and Physical Sciences Research Council
640 (EP/G03768X/1) and the RAEng through a Newton Fellowship grant (NRCP/1415/176).
641 The authors would like to acknowledge Prof. Rod Scott and Dr Philippe Mozzanega in
642 the Algal Research Group at the University of Bath, for the provision of the wastewater-
643 derived microalgae, and to Michael J. Allen and Tracey Beacham at the Plymouth
644 Marine Laboratory for conducting the biochemical analysis of the biomass. The data
645 repository can be freely accessed at (<https://doi.org/10.15125/BATH-00304>).

646 **References**

- 647 1. S. Raikova, C. D. Le, J. L. Wagner, V. P. Ting and C. J. Chuck, in *Biofuels for Aviation -*
648 *Feedstocks, Technology and Implementation*, ed. C. J. Chuck, Elsevier, London, 2016.
- 649 2. Elliott, D.C., Review of recent reports on process technology for thermochemical
650 conversion of whole algae to liquid fuels. *Algal Res.*, 2016. 13: p. 255-263.

- 651 3. D. López Barreiro, W. Prins, F. Ronsse and W. Brilman, Hydrothermal liquefaction (HTL)
652 of microalgae for biofuel production: state of the art review and future prospects.
653 Biomass Bioenerg. 2013, 53, 113-127.
- 654 4. L. Xu, D. W. Wim Brilman, J. A. Withag, G. Brem and S. Kersten, Assessment of a dry
655 and a wet route for the production of biofuels from microalgae: energy balance analysis.
656 Bioresource Technol., 2011, 102, 5113-5122.
- 657 5. P. Biller, A. B. Ross, S. C. Skill, A. Lea-Langton, B. Balasundaram, C. Hall, R. Riley and
658 C. A. Llewellyn. Nutrient recycling of aqueous phase for microalgae cultivation from the
659 hydrothermal liquefaction process. Algal Res., 2012, 1, 70-76.
- 660 6. U. Jena, N. Vaidyanathan, S. Chinnasamy and K. C. Das, Evaluation of microalgae
661 cultivation using recovered aqueous co-product from thermochemical liquefaction of
662 algal biomass. Bioresoure Technol., 2011, 102, 3380-3387.
- 663 7. L. Garcia Alba, C. Torri, D. Fabbri, S. R. A. Kersten and D. W. F. Brilman, Microalgae
664 growth on the aqueous phase from hydrothermal liquefaction of the same microalgae
665 Chem. Eng. J. 2013, 228, 214-223.
- 666 8. C. J. Chuck, J. L. Wagner and R. W. Jenkins, in Chemical Processes for a Sustainable
667 Future, eds. T. M. Letcher, J. L. Scott and D. A. Patterson, Royal Society of Chemistry,
668 Cambridge, 2015, ch. 16, pp. 425-442.
- 669 9. Elliott, D.C., et al., Hydrothermal liquefaction of biomass: developments from batch to
670 continuous process. Bioresoure Technol., 2015. 178: p. 147-56.
- 671 10. J. L. Faeth, P. J. Valdez and P. E. Savage. Fast hydrothermal liquefaction of
672 Nannochloropsis sp. to produce biocrude. Energ. Fuel. 2013, 27, 1391-1398.
- 673 11. L. Garcia Alba, C. Torri, C. Samori, J. van der Spek, D. Fabbri, S. R. A. Kersten and D.
674 W. F. Brilman. Hydrothermal treatment (HTT) of microalgae: evaluation of the process
675 as conversion method in an algae biorefinery concept. Energ. Fuel., 2012, 26, 642-657.
- 676 12. A. Cole, Y. Dinburg, B. S. Haynes, Y. He, M. Herskowitz, C. Jazrawi, M. Landau, X.
677 Liang, M. Magnusson, T. Maschmeyer, A. F. Masters, N. Meiri, N. Neveux, R. de Nys, N.
678 Paul, M. Rabaev, R. Vidruk-Nehemya and A. K. L. Yuen. From macroalgae to liquid fuel
679 via waste-water remediation, hydrothermal upgrading, carbon dioxide hydrogenation and
680 hydrotreating. Energy Environ. Sci., 2016, 9, 1828-1840.
- 681 13. J. L. Garcia-Moscoso, W. Obeid, S. Kumar and P. G. Hatcher, Flash hydrolysis of
682 microalgae (*Scenedesmus* sp.) for protein extraction and production of biofuels
683 intermediates. J. Supercrit. Fluid., 2013, 82, 183-190.

- 684 14. P. Biller, B. K. Sharma, B. Kunwar and A. B. Ross. Hydroprocessing of bio-crude from
685 continuous hydrothermal liquefaction of microalgae. *Fuel*, 2015, 159, 197-205.
- 686 15. B. Patel and K. Hellgardt. Hydrothermal upgrading of algae paste in a continuous flow
687 reactor. *Bioresource Technol.*, 2015, 191, 460-468.
- 688 16. C. Jazrawi, P. Biller, A. B. Ross, A. Montoya, T. Maschmeyer and B. S. Haynes. Pilot
689 plant testing of continuous hydrothermal liquefaction of microalgae. *Algal Res.*, 2013, 2,
690 268-277.
- 691 17. D. C. Elliott, T. R. Hart, A. J. Schmidt, G. G. Neuenschwander, L. J. Rotness, M. V.
692 Olarte, A. H. Zacher, K. O. Albrecht, R. T. Hallen and J. E. Holladay. Process
693 development for hydrothermal liquefaction of algae feedstocks in a continuous-flow
694 reactor. *Algal Res.*, 2013, 2, 445-454.
- 695 18. D. L. Barreiro, B. R. Gómez, U. Hornung, A. Kruse and W. Prins. Hydrothermal
696 liquefaction of microalgae in a continuous stirred-tank reactor. *Energ. Fuel.*, 2015, 29,
697 6422-6432.
- 698 19. C. M. Beal, L. N. Gerber, D. L. Sills, M. E. Huntley, S. C. Machesky, M. J. Walsh, J. W.
699 Tester, I. Archibald, J. Granados and C. H. Greene. Algal biofuel production for fuels and
700 feed in a 100-ha facility: A comprehensive techno-economic analysis and life cycle
701 assessment. *Algal Res.*, 2015, 10, 266-279.
- 702 20. N. D. Orfield, Doctor of Philosophy PhD Thesis, University of Michigan, 2013.
- 703 21. R. Sayre. Microalgae: the potential for carbon capture. *BioScience*, 2010, 60, 722-727.
- 704 22. M. K. Lam and K. T. Lee. Microalgae biofuels: a critical review of issues, problems and
705 the way forward. *Biotechnol. Adv.*, 2012, 30, 673-690.
- 706 23. M. K. Lam, K. T. Lee and A. R. Mohamed. Current status and challenges on microalgae-
707 based carbon capture. *Int. J. Greenhouse Gas Control*, 2012, 10, 456-469.
- 708 24. S. Raikova, H. Smith-Baedorf, R. Bransgrove, O. Barlow, F. Santomauro, J. L. Wagner,
709 M. J. Allen, C. G. Bryan, D. Sapsford and C. J. Chuck. Assessing hydrothermal
710 liquefaction for the production of bio-oil and enhanced metal recovery from microalgae
711 cultivated on acid mine drainage. *Fuel Process. Technol.*, 2016, 142, 219-227.
- 712 25. R. J. Craggs, S. Heubeck, T. J. Lundquist and J. R. Benemann. Algal biofuels from
713 wastewater treatment high rate algal ponds. *Water Sci Technol.*, 2011, 63, 660-665.
- 714 26. A. Kumar, S. Ergas, X. Yuan, A. Sahu, Q. Zhang, J. Dewulf, F. X. Malcata and H. van
715 Langenhove. Enhanced CO₂ fixation and biofuel production via microalgae: recent
716 developments and future directions. *Trends Biotechnol.*, 2010, 28, 371-380.

- 717 27. Aquastat, Food and Agriculture Organization of the United Nations, 2014. Available
718 from: <http://www.fao.org/nr/water/aquastat/wastewater/index.stm> [28/08/2014].
- 719 28. Cogan, M. and B. Antizar-Ladislao, The ability of macroalgae to stabilise and optimise
720 the anaerobic digestion of household food waste. *Biomass Bioenerg.*, 2016. 86: p. 146-
721 155.
- 722 29. K. A. C. C. Taylor. A modification of the phenol/sulfuric acid assay for total
723 carbohydrates giving more comparable absorbances *Appl. Biochem. Biotech.*, 1995, 53,
724 207-214.
- 725 30. E. T. Kostas, D. A. White, C. Du and D. J. Cook, Selection of yeast strains for bioethanol
726 production from UK seaweeds. *J. Appl. Phycol.*, 2016, 28, 1427-1441.
- 727 31. J. Wagner, R. Bransgrove, T. A. Beacham, M. J. Allen, K. Meixner, B. Drosig, V. P. Ting
728 and C. J. Chuck. Co-production of bio-oil and propylene through the hydrothermal
729 liquefaction of polyhydroxybutyrate producing cyanobacteria. *Bioresource Technol.*,
730 2016, 207, 166-174.
- 731 32. F. Mariotti, D. Tome and P. P. Mirand. Converting nitrogen into protein—beyond 6.25
732 and Jones' factors *Crit. Rev. Food Science Nutrition*, 2008, 48, 177-184.
- 733 33. A.B. Ross, J.M. Jones, M.L. Kubacki, T. Bridgeman, Classification of macroalgae as fuel
734 and its thermochemical behaviour. *Bioresource Technol.*, 2008. 99(14): p. 6494-504.
- 735 34. X. Cheng, M. D. Ooms and D. Sinton, Biomass-to-biocrude on a chip via hydrothermal
736 liquefaction of algae. *Lab on a Chip*, 2016, 16, 256-260.
- 737 35. C. Torri, L. Garcia Alba, C. Samori, D. Fabbri and D. W. F. Brillman. Hydrothermal
738 treatment (HTT) of microalgae: detailed molecular characterization of HTT oil in view of
739 HTT mechanism elucidation. *Energ. Fuel.*, 2012, 26, 658-671.
- 740 36. J. L. Faeth, P. E. Savage, J. M. Jarvis, A. M. McKenna and P. E. Savage.
741 Characterization of products from fast and isothermal hydrothermal liquefaction of
742 microalgae. *AIChE J.* 2016, 62, 815-828.
- 743 37. C. Tian, Z. Liu, Y. Zhang, B. Li, W. Cao, H. Lu, N. Duan. Hydrothermal liquefaction of
744 harvested high-ash low-lipid algal biomass from Dianchi Lake: effects of operational
745 parameters and relations of products. *Bioresource Technol.*, 2015. 184: p. 336-43.
- 746 38. W.T. Chen, Y. Zhang, J. Zhang, G. Yu, L.C. Schideman. Hydrothermal liquefaction of
747 mixed-culture algal biomass from wastewater treatment system into bio-crude oil.
748 *Bioresource Technol.*, 2014. 152: p. 130-9.
- 749 39. S. S. Toor, L. Rosendahl and A. Rudolf, Hydrothermal liquefaction of biomass: a review
750 of subcritical water technologies. *Energy*, 2011, 36, 2328-2342.

751 40. W. Yang, X. Li, Z. Li, C. Tong and L. Feng. Understanding low-lipid algae hydrothermal
752 liquefaction characteristics and pathways through hydrothermal liquefaction of algal
753 major components: Crude polysaccharides, crude proteins and their binary
754 mixtures. *Bioresource Technol.*, 2015, 196, 99-108.
755
756

757 **Figure legends**

758

759 Table 1: Proximate and ultimate analysis of wastewater algae

760

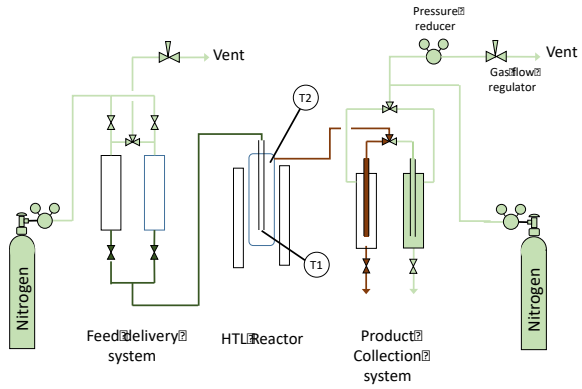
761 Figure 1: Process schematic for continuous HTL system

762 Figure 2: Effect of reaction temperature on the batch conversion of wastewater-derived algae; (a)
763 overall product distribution, (b) CHN retention in biocrude, (c) CN retention in aqueous phase,
764 calculated from TOC and TN analysis, with the results from ammonium ion analysis superimposed
765 as orange markers. Error bars represent the standard deviations of three repeats

766 Figure 3: Effect of heating rate on the batch conversion of wastewater-derived algae; (a) overall
767 product distribution, (b) CHN retention in biocrude, (c) CN retention to aqueous-phase from TOC
768 and TN analysis, with the results from ammonium ion analysis superimposed as orange markers.
769 Error bars represent the standard deviations of three repeats.

770 Figure 4: Effect of reaction temperature on the continuous liquefaction of wastewater algae; (a)
771 overall product distribution, (b) CHN retention in bio-crude, (c) CN retention to aqueous-phase
772 from TOC and TN analysis, with the results from ammonium ion analysis superimposed as orange
773 markers. Error bars represent standard deviation of two repeats conducted at 320 °C.

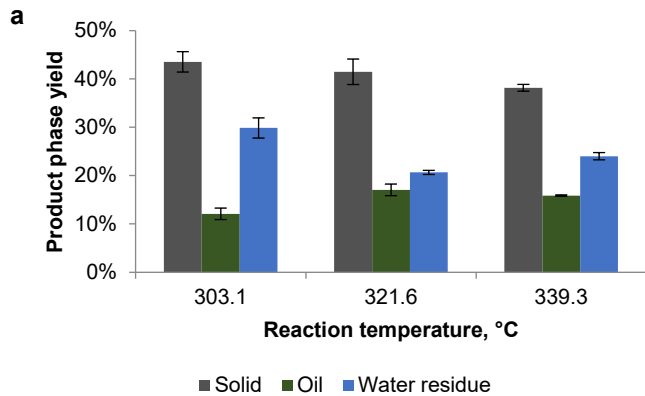
774 Figure 5: Effect of feed flowrate on the continuous liquefaction of wastewater algae; (a) overall
775 product distribution, (b) CHN retention in bio-crude, (c) CN retention to aqueous-phase from
776 TOC and TN analysis, with the results from ammonium ion analysis superimposed as orange
777 markers. Error bars represent standard deviation of two repeats conducted at highest flowrate.
778



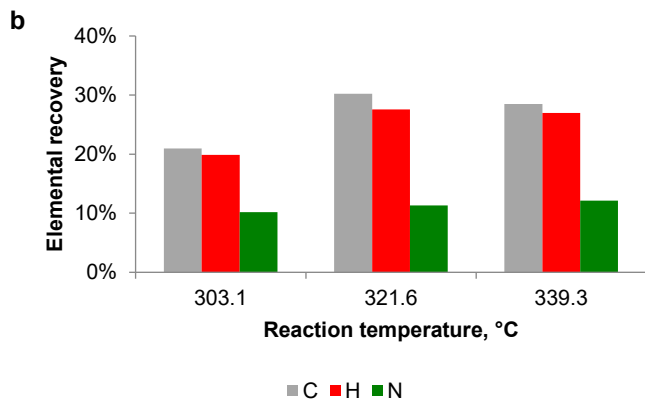
779

780 **Figure 1: Process schematic for continuous HTL system**

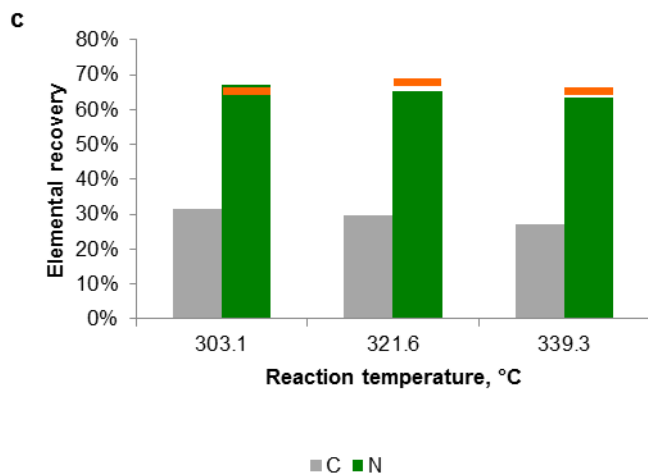
781



782



783



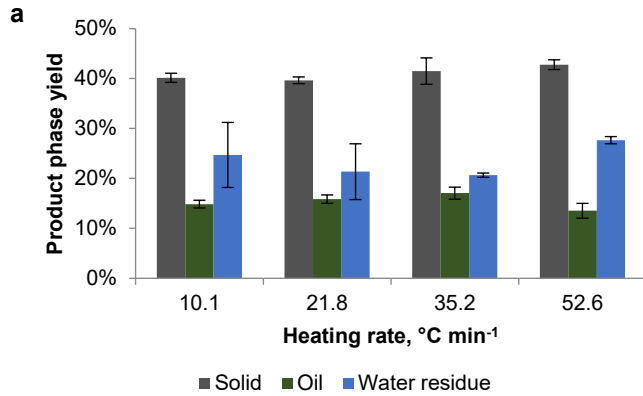
784

785

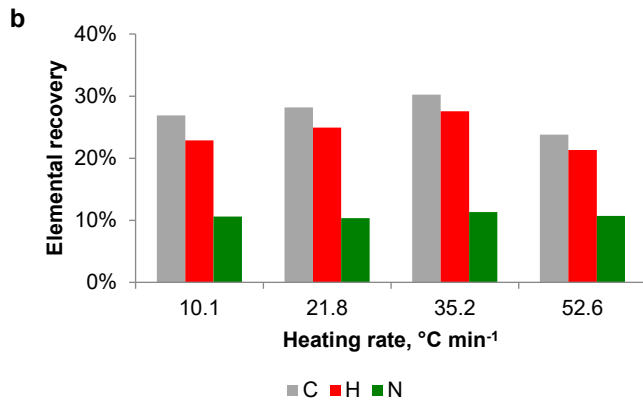
786 **Figure 2: Effect of reaction temperature on the batch conversion of wastewater-derived algae; (a)**
 787 **overall product distribution, (b) CHN retention in biocrude, (c) CN retention in aqueous phase,**
 788 **calculated from TOC and TN analysis, with the results from ammonium ion analysis superimposed**
 789 **as orange markers. Error bars represent the standard deviations of three repeats.**

790

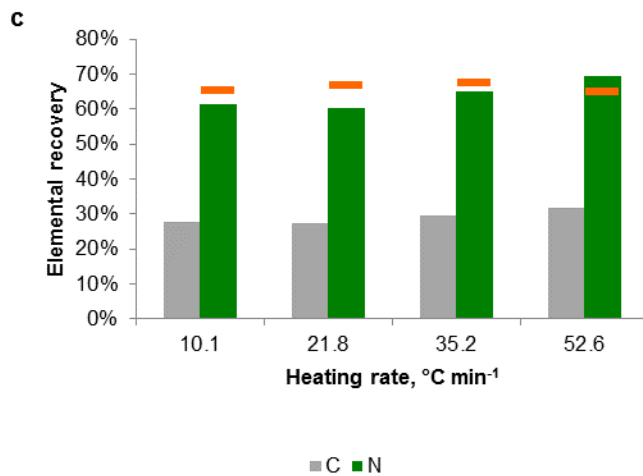
791



792



793



794

795

796

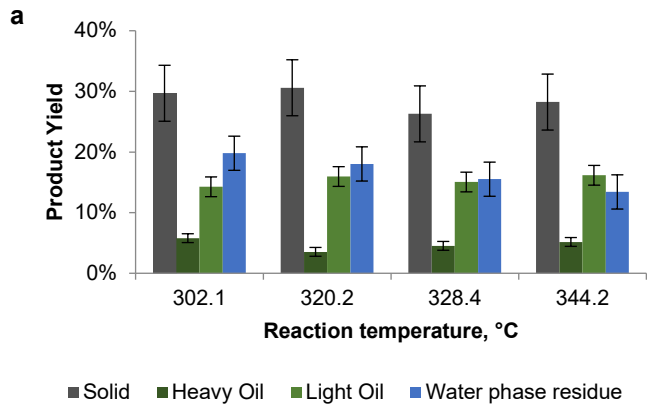
797

798

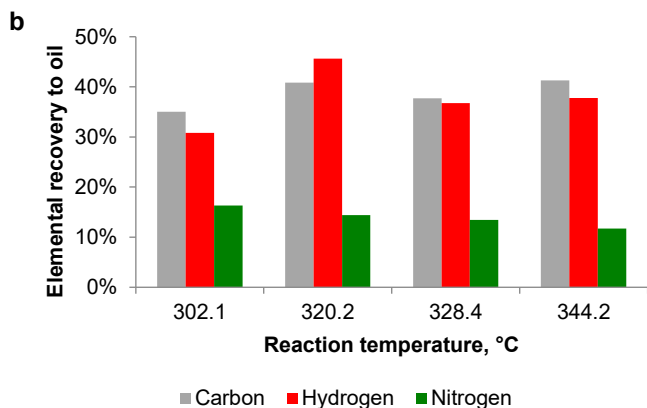
Figure 3: Effect of heating rate on the batch conversion of wastewater-derived algae; (a) overall product distribution, (b) CHN retention in biocrude, (c) CN retention to aqueous-phase from TOC and TN analysis, with the results from ammonium ion analysis superimposed as orange markers. Error bars represent the standard deviations of three repeats.

799

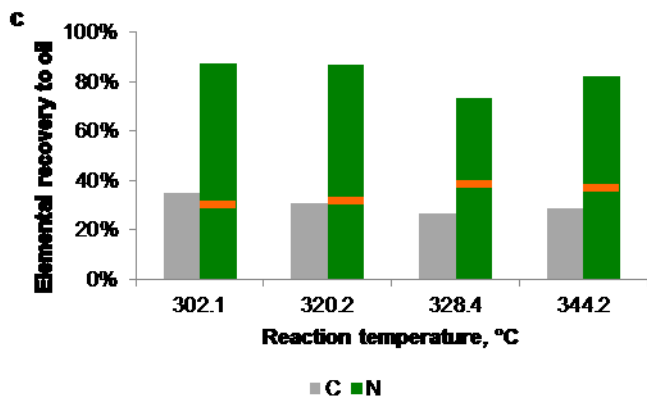
800



801



802



803

804

805

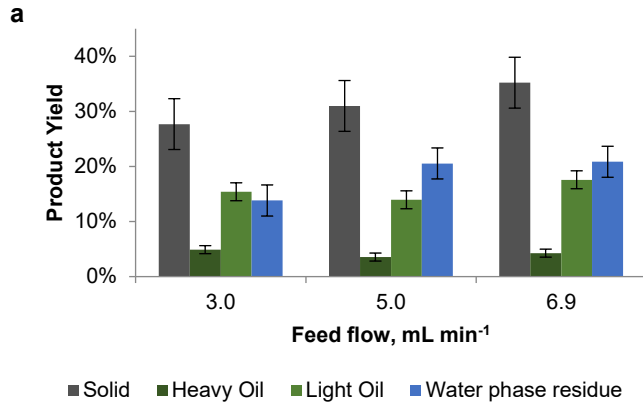
806

807

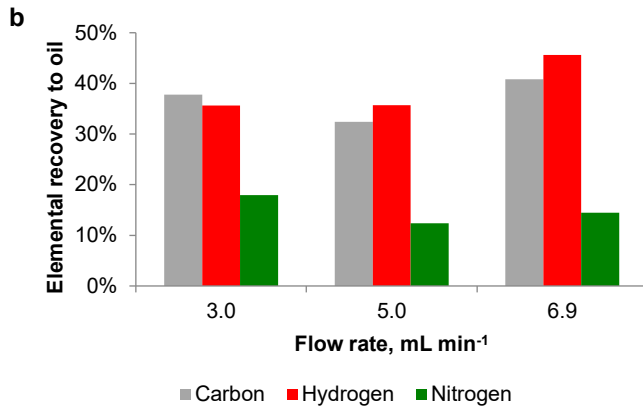
Figure 4: Effect of reaction temperature on the continuous liquefaction of wastewater algae; (a) overall product distribution, (b) CHN retention in bio-oil, (c) CN retention to aqueous-phase from TOC and TN analysis, with the results from ammonium ion analysis superimposed as orange markers. Error bars represent standard deviation of two repeats conducted at 320 °C.

808

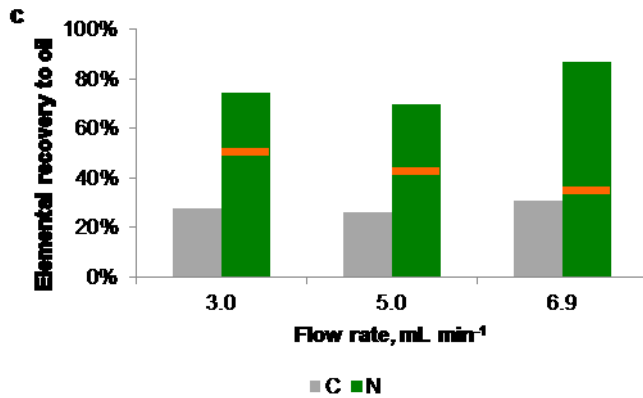
809



810



811



812

813

814

815

816

Figure 5: Effect of feed flowrate on the continuous liquefaction of wastewater algae; (a) overall product distribution, (b) CHN retention in bio-oil, (c) CN retention to aqueous-phase from TOC and TN analysis, with the results from ammonium ion analysis superimposed as orange markers. Error bars represent standard deviation of two repeats conducted at highest flowrate.

817

818

819

820

821

